Boletín de la Sociedad Española de Cerámica y Vidrio
Vol 52, 2, 93-97, Marzo-Abril 2013 ISSN 0366-3175. eISSN 2173-0431.
doi: 10.3989/cyv.122013

BOLETIN DE LA SOCIEDAD ESPAÑOLA DE
Cerámica y Vidrio
A R T I C U L O

Effect of Ag additions on the $Bi_{1.6}Pb_{0.4}Sr_2Co_{1.8}O_x$ thermoelectric properties

J. C. DIEZ[1], SH. RASEKH[1], G. CONSTANTINESCU[1], M. A. TORRES[2], M. A. MADRE[1], A. SOTELO[1]

[1]Instituto de Ciencia de Materiales de Aragón (CSIC-Universidad de Zaragoza), Mª de Luna, 3. 50018 Zaragoza, Spain.
[2]Departamento de Ingeniería de Diseño y Fabricación. Universidad de Zaragoza, Mª de Luna, 3. 50018 Zaragoza, Spain.

$Bi_{1.6}Pb_{0.4}Sr_2Co_{1.8}O_x$ thermoelectric ceramics with small Ag additions (0, 1, and 3 wt.%) have been successfully produced by a sol-gel method via nitrates. Microstructure has shown a reduction on the amount of secondary phases and an increase on the bulk density with increasing Ag contents. The microstructural evolution, as a function of Ag content, is confirmed with the electrical resistivity values which show an important decrease for the 3 wt.% Ag samples, leading to maximum power factor values of about 0.025 mW/K².m at room temperature, which is about two times higher than the obtained for the Ag-free sintered samples.

Keywords: Processing, Electrical properties, Microstructure, Thermopower, Cobaltites.

Efecto de la adición de Ag additions en las propiedades termoeléctricas del $Bi_{1.6}Pb_{0.4}Sr_2Co_{1.8}O_x$

Se han preparado cerámicas termoeléctricas de composición $Bi_{1.6}Pb_{0.4}Sr_2Co_{1.8}O_x$ con pequeñas adiciones de Ag (0, 1, y 3 % en peso) por medio de un método sol-gel a partir de los nitratos metálicos. La microestructura ha mostrado una reducción de la cantidad de fases secundarias y un aumento de la densidad del material al aumentar la cantidad de Ag. La evolución microestructural, en función del contenido de Ag, se ha confirmado con los valores de la resistividad eléctrica que muestra una reducción importante para las muestras con 3 % en peso de Ag, lo que lleva a alcanzar valores máximos del factor de potencia de alrededor de 0.025 mW/K².m a temperatura ambiente, que es dos veces mayor que el obtenido para muestras sinterizadas sin Ag.

Palabras clave: Procesamiento, Propiedades eléctricas, Microestructura, Termopower, Cobaltitas.

1. INTRODUCTION

Thermoelectric (TE) materials possessing high energy conversion efficiency are necessary in order to be applied in practical electric power generation systems. Thermoelectric energy conversion has very important advantages to harvest waste heat in a wide number of industrial applications. Moreover, it can be used to transform solar energy into electricity at lower cost than photovoltaic energy [1]. The conversion efficiency of such materials is quantified by the dimensionless figure of merit ZT, which is defined as $TS^2/\rho\kappa$ (in which S^2/ρ is also called power factor, PF), where S is the Seebeck coefficient (or thermopower), ρ the electrical resistivity, κ the thermal conductivity, and T is the absolute temperature [2]. As a consequence, an adequate TE material for practical applications must involve, therefore, high thermopower and low electrical resistivity, with low thermal conductivity.

The discovery of large thermoelectric power in Na_xCoO_2 [3], which was found to possess a high ZT value of about 0.26 at 300K, has opened a broad research field and from that moment on, great efforts have been devoted to explore new cobaltite families with high thermoelectric performances. Some other layered cobaltites, such as misfit $[Ca_2CoO_3][CoO_2]_{1.62}$, $[Bi_{0.87}SrO_2]_2[CoO_2]_{1.82}$ and $[Bi_2Ca_2O_4][CoO_2]_{1.65}$ were also found to exhibit attractive thermoelectric properties [4-8]. In these systems, the crystal structure is formed by two different layers, showing an alternate stacking of a common conductive CdI_2-type CoO_2 layer with a two-dimensional triangular lattice and a block layer, composed of insulating rock-salt-type (RS) layers. Both sublattices (RS block and CdI_2-type CoO_2 layer) possess common a- and c-axis lattice parameters and β angles but different b-axis length, causing a misfit along the b-direction [9,10].

One of the main factors affecting the thermoelectric performances of this kind of materials is the electrical resistivity which should be maintained as low as possible. The resistivity values in ceramic materials are influenced by a number of different parameters as content and distribution of secondary phases, porosity, oxygen content, etc. As a consequence, many different synthetic methods have been used in order to synthesize thermoelectric and other layered ceramic materials [11-18]. On the other hand, layered cobaltites are materials with a strong crystallographic anisotropy; therefore the alignment of plate-like grains by mechanical and/or chemical processes has been studied to attain macroscopic properties comparable

to those obtained on single crystals mainly due to the electrical resistivity decrease. Some techniques have been shown to be adequate to obtain a good grain orientation in several oxide ceramic systems, such as templated grain growth (TGG) [10], sinter-forging [19], spark plasma sintering [20], or directional growth from the melt [21,22]. Other possibilities arising from the crystallographic structure of these materials are the cationic substitutions in the RS layer, which can change the misfit relationship between the two layers and, as a consequence, modifying the values of the thermopower [7]. From this point of view, it is clear that this kind of substitutions can be useful in order to improve thermoelectric performances of ceramic materials [19], as it is reported for the substitution of Gd and Y for Ca [23], or Pb for Bi [24-26]. Moreover, metallic Ag additions have also shown to improve, in an important manner, the mechanical and electric properties of this system [27] and other similar materials [28] which nearly do not react with Ag, as it has been found in some phase diagram studies [29].

Taking into account these previously discussed effects, the aim of this work is producing high performance TE materials by the addition of small amounts of metallic Ag, determined in previous works [27], to the optimally Pb doped Bi-Sr-Co-O compound studied in previous works [24,30].

2. EXPERIMENTAL

The initial $Bi_{1.6}Pb_{0.4}Sr_2Co_{1.8}O_x$ polycrystalline ceramics with small amounts of silver (0, 1, and 3 wt.% Ag) were prepared from commercial $Bi(NO_3)_3 \bullet 5H_2O$ (≥98 %, Aldrich), PbO (Aldrich, ≥ 99 %), $SrCO_3$ (98.5 %, Panreac), $Co(NO_3)_2 \bullet 6H_2O$ (98 %, Panreac), and metallic Ag (99 %, Aldrich) powders by a sol-gel via nitrates method described in detail elsewhere [31]. They were weighed in the appropriate proportions and dissolved in a mixture of distilled water and concentrated HNO_3 (analysis grade, Panreac) of about 50 vol.% of each component, leading to a clear pink solution. Citric acid (99.5 %, Panreac), and ethylene glycol (99 %, Panreac), were added to this solution in the adequate proportions and stirred until all the products were dissolved. Evaporation of the solvent was performed slowly, in a hot plate at around 50-75 ºC, in order to decompose the nitric acid excess which allows the polymerization reaction between ethylene glycol and citric acid, forming a pink gel [32]. Once the polymerization has been finished, the temperature was raised to evaporate the remaining water and the unreacted ethylene glycol. At the same time, the nitrates are decomposed and nitrogen oxides are released, leaving the organometallic coordination compound. This complex was then decomposed (slow self combustion) by heating at 350-400 ºC for 1 h, producing very fine and homogeneous powders which were mechanically ground and calcined at 750 and 800 °C for 12 h, with an intermediate grinding, to totally decompose the $SrCO_3$ produced in the coordination compound combustion. The resulting powder was uniaxially pressed in form of parallelepipeds (~14 mm x 2 mm x 3 mm) under an applied pressure of about 400 Mpa. The compact materials were then sintered at 810 ºC under air during 24 h with furnace cooling, which are the best conditions for the pure composition [12].

The structural identification of all the samples was performed by powder XRD utilizing a Rigaku D/max-B X-ray powder diffractometer (CuKα radiation) with 2θ ranging between 10 and 70 degrees. Microstructural observations were performed on polished samples using a Field Emission Scanning Electron Microscope (FESEM, Carl Zeiss Merlin) fitted with energy dispersive spectrometry (EDS) analysis. Micrographs of these samples have been recorded to analyze the different phases and their distribution. From these pictures, an estimation of the amount of the different phases has been performed using Digital Micrograph software. Moreover, apparent density measurements have been performed in several samples for each composition.

Steady-state simultaneous measurements of resistivity and thermopower were determined by the standard dc four-probe technique in a LSR-3 apparatus (Linseis GmbH) between 50 and 650 ºC under He atmosphere. From these data, PF values as a function of temperature were calculated in order to evaluate the final samples performances.

3. RESULTS AND DISCUSSION

Powder XRD patterns for all $Bi_{1.6}Pb_{0.4}Sr_2Co_{1.8}O_x$ samples with different amounts of Ag are plotted (from 10 to 40° for clarity) in Fig. 1. They show very similar patterns where the most intense peaks correspond to the misfit cobaltite $Bi_{1.6}Pb_{0.4}Sr_2Co_{1.8}O_x$ phase, in agreement with previous reported data [24,33]. From this figure, it is clear that the cobaltite phase appears as the major one, independently of Ag content. Peaks marked with a ● in the plot correspond to the Co-free $Bi_{0.75}Sr_{0.25}O_{1.375}$ secondary phase [34], and the * indicates the (111) peak of Si, used for reference. Moreover, for the samples with 1 and 3wt.% Ag, a new peak appears in the XRD plots at around 38 degrees, which corresponds to the metallic Ag (111) plane (indicated by ■) [35]. This peak also indicates that Ag does not react with the thermoelectric ceramic, leading

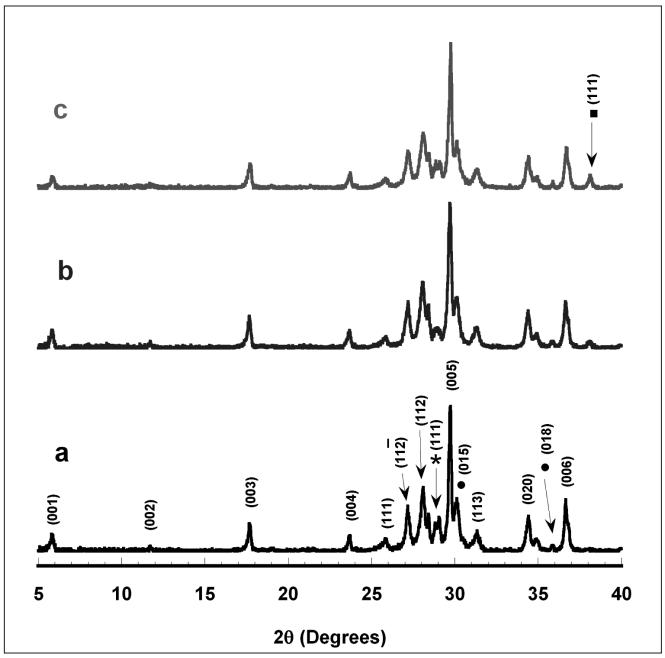

Figure 1. Powder XRD diagrams for the $Bi_{1.6}Pb_{0.4}Sr_2Co_{1.8}O_x$ sintered samples with a) 0; b) 1; and c) 3 wt.% Ag. Crystallographic planes have been indicated on the peaks corresponding to the $Bi_{1.6}Pb_{0.4}Sr_2Co_{1.8}O_x$ phase. Other phases are indicated by symbols: ● Co-free $Bi_{0.75}Sr_{0.25}O_{1.375}$ secondary phase; ■ Ag; and * Si (111) peak used as reference.

Bol. Soc. Esp. Ceram. Vidr. Vol 52. 2, 93-97, Marzo-Abril 2013. ISSN 0366-3175. eISSN 2173-0431. doi: 10.3989/cyv.122013

to the formation of a ceramic matrix composite with metallic particles distributed inside the matrix, as observed in similar ceramic systems [28,36,37].

Scanning electron microscopy has been performed on polished transversal sections of all samples after the sintering process. The microstructural evolution of samples, as a function of Ag content, can be easily observed in Fig. 2 where representative micrographs, recorded with backscattered electrons, of all samples are presented. In these views, it can be clearly seen that porosity decreases when Ag is added to the samples. This is in agreement with the apparent density measurements performed on the sintered samples, which show an increase of density when the Ag amount is increased. The mean values are 4.89 gr/cm^3 for the pure $Bi_{1.6}Pb_{0.4}Sr_2Co_{1.8}O_x$ samples, while they increase to 5.22 and 5.70 gr/cm^3 for the 1 and 3 wt.% Ag-containing samples after subtracting the Ag contribution to the total density. This effect can be due to the formation of a eutectic phase in the $Bi_{1.6}Pb_{0.4}Sr_2Co_{1.8}O_x$/Ag pseudobinary system, as it was previously reported for relatively similar systems [29]. As a consequence, melting point is decreased which favours further densification than the produced in samples without Ag.

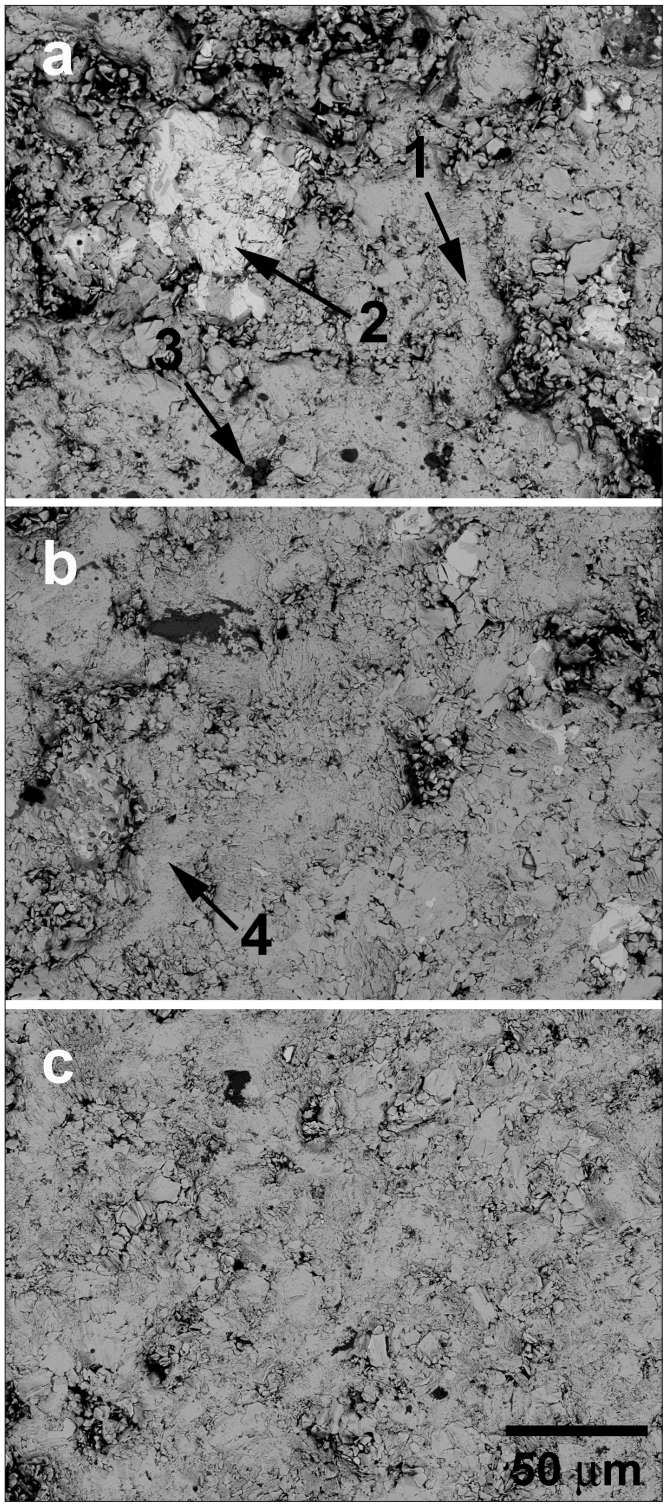

Figure 2. Scanning electron micrographs from transversal polished samples $Bi_{1.6}Pb_{0.4}Sr_2Co_{1.8}O_x$ with different Ag contents with backscattered electrons: a) 0; b) 1; and c) 3 wt.%. The contrasts corresponding to the different phases are indicated by arrows, 1) $Bi_{1.6}Pb_{0.4}Sr_2Co_{1.8}O_x$; 2) $Bi_3Sr_2O_y$; 3) CoO; and 4) Ag.

Moreover three main contrasts can be identified in these micrographs. Each one correspond to a different phase, grey contrast (#1) associated by EDX to the thermoelectric $Bi_{1.6}Pb_{0.4}Sr_2Co_{1.8}O_x$ phase, and white (#2) and dark grey (#3) ones to the Bi_3SrO_y and CoO secondary phases, respectively. Even if CoO phase has not been identified in the XRD patterns, the proportion and the other present phases are in agreement with the previously discussed XRD data. In this figure, it can also be observed that in Ag-added samples the amount and size of these secondary phases are reduced. Moreover, a new grey contrast appears, corresponding to the metallic Ag. It is very similar to the thermoelectric phase but it can be distinguished by the nearly spherical shape of Ag particles (#4 in Fig. 2b). In order to estimate the amount of each phase in the bulk materials, several micrographs have been analysed for each composition. The approximate content of these secondary phases is about 7 vol.% of $Bi_3Sr_2O_y$ and 8 vol.% of CoO for the pure samples, which are reduced to around 3 and 5 vol.% for the 1 wt.%Ag ones, and 1 and 3 vol.% found in the 3 wt.%Ag samples, following the same trends found in previously published works on textured materials [38].

The temperature dependence of the electrical resistivity as a function of the Ag content is represented in Fig. 3. As it can

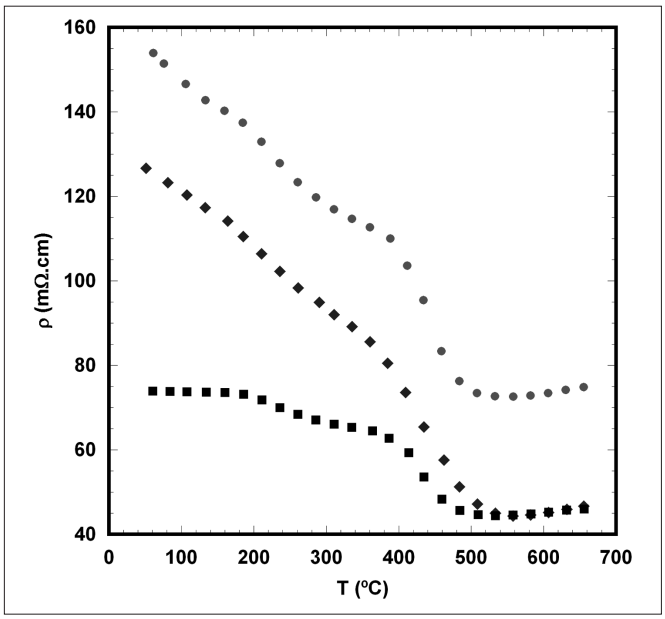

Figure 3. Temperature dependence of the electrical resistivity for textured $Bi_{1.6}Pb_{0.4}Sr_2Co_{1.8}O_x$ with different Ag contents. ● 0; ◆ 1; and ■ 3 wt.%.

be easily seen, the ρ(T) curves show very similar behaviour for all samples. All curves display a semiconducting-like behaviour ($d\rho/dT < 0$) from room temperature to about 550 ºC and a slightly metallic-like one ($d\rho/dT > 0$) at higher temperatures. On the other hand, when increasing Ag contents, a significant reduction on the resistivity values at room temperature, is produced. This evolution of the electrical resistivity is consistent with the reduction of the secondary phases content already mentioned in the microstructure discussion (see Fig. 2) and the increase on the samples density already described in the apparent density measurements. The minimum resistivity value at room temperature, ~ 75 mΩ.cm, is obtained for samples with 3 wt.% Ag, while for the 0 and 1 wt.% Ag is about two times higher, 155 and 125 mΩ.cm, respectively.

Fig. 4 displays the variation of the Seebeck coefficient as a function of temperature for all the samples. In this figure, it is clear that the sign of the Seebeck coefficient is positive for the whole measured temperature range, which confirms a conduction mechanism predominantly governed by holes. The values increase almost linearly with temperature in all the measured range, with very similar values for all the samples. This is a clear indication that these small amounts of Ag do not affect thermopower values, as observed in annealed textured samples without Pb [27]. In all cases, the room temperature values are higher than the measured in single crystals with similar composition without Ag (about 100 μV/K) [39].

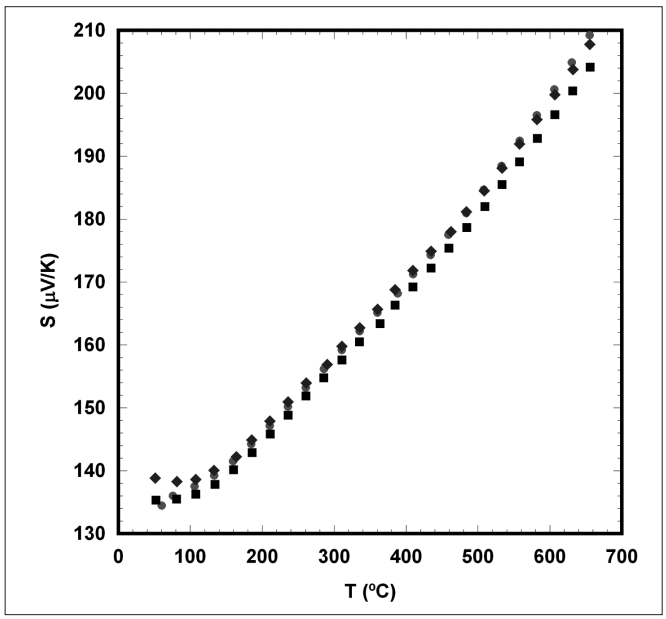

Figure 4. Temperature dependence of the Seebeck coefficient for textured $Bi_{1.6}Pb_{0.4}Sr_2Co_{1.8}O_x$ with different Ag contents. ● 0; ◆ 1; and ■ 3 wt.%.

In order to evaluate the thermoelectric performances of the sintered ceramic materials, variation of Power Factor with temperature has been calculated from the resistivity and Seebeck coefficient values and displayed, as a function of the Ag content, in Fig. 5. As it was found in the Seebeck coefficient measurements, PF increases with temperature in all the measured range. Moreover, the values at room temperature increase with Ag content, due to the decrease on the electrical resistivity values. The minimum value, at room temperature, of about 0.025 mW/K².m for the 3wt.% samples, is lower than the obtained on in-plane measurements performed in single crystals without Ag (~ 0.2 mW/K².m) [40], but higher than the obtained ones in pure sintered $Bi_2Sr_2Co_{1.8}O_z$ (~ 0.017 mW/K².m) [12]. Moreover, it is more than two times higher than the obtained for the pure $Bi_{1.6}Pb_{0.4}Sr_2Co_{1.8}O_x$. This result indicates that small Ag additions can be very useful in order to strongly reduce electrical resistivity and, as a consequence, raising the thermoelectric performances of these ceramic materials.

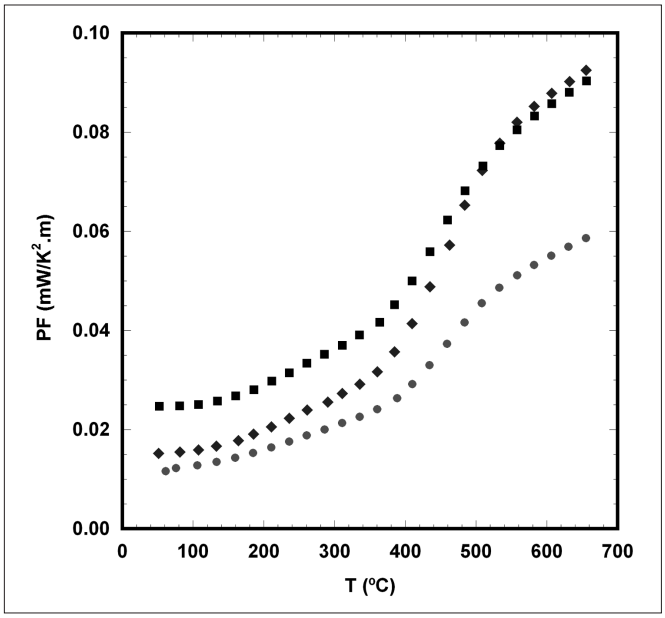

Figure 5. Temperature dependence of the power factor for textured $Bi_{1.6}Pb_{0.4}Sr_2Co_{1.8}O_x$ with different Ag contents. ● 0; ◆ 1; and ■ 3 wt.%.

4. CONCLUSIONS

This paper demonstrates that $Bi_{1.6}Pb_{0.4}Sr_2Co_{1.8}O_x$ thermoelectric materials with small Ag additions (0, 1, and 3 wt.%) can be produced successfully by the sol-gel method. It has been determined that Ag addition significantly reduces the amount of secondary phases and increases the apparent density of the samples. Moreover, the electrical resistivity data clearly indicated that Ag produces an important reduction of their electrical resistivity without modifying the Seebeck coefficient values. All these factors lead to a raise in the Power Factor of about two times, at room temperature, compared with the pure $Bi_{1.6}Pb_{0.4}Sr_2Co_{1.8}O_x$.

ACKNOWLEDGEMENTS

This research has been supported by the Spanish Ministry of Science and Innovation (Project MAT2008-00429) and the Universidad de Zaragoza (Project UZ2011-TEC-03). The authors wish to thank the Gobierno de Aragón (Consolidated Research Groups T87 and T12) for financial support and to C. Gallego, C. Estepa and J. A. Gomez for their technical assistance. Sh. Rasekh acknowledges a JAE-PreDoc2010 grant from the CSIC.

REFERENCES

1. W. Liu, X. Yan, G. Chen, Z. Ren. Recent advances in thermoelectric nanocomposites. Nano Energy 1 (1), 42-56 (2012).
2. D.M. Rowe, in: D.M. Rowe (Ed.), Thermoelectrics Handbook: Macro to Nano, 1st edn, CRC Press, Boca Raton, FL, 2006, pp. 1-3–1-7.
3. I. Terasaki, Y. Sasago, K. Uchinokura. Large thermoelectric power in $NaCo_2O_4$ single crystals. Phys. Rev. B 56 (20), 12685–12687 (1997).
4. R. Funahashi, I. Matsubara, H. Ikuta, T. Takeuchi, U. Mizutani, S. Sodeoka. An oxide single crystal with high thermoelectric performance in air. Jpn. J. Appl. Phys. 39 (11B), L1127–L1129 (2000).
5. A. C. Masset, C. Michel, A. Maignan, M. Hervieu, O. Toulemonde, F. Studer, B. Raveau, J. Hejtmanek. Misfit-layered cobaltite with an anisotropic giant magnetoresistance: $Ca_3Co_4O_9$. Phys. Rev. B 62 (1), 166–175 (2000).
6. H. Leligny, D. Grebille, O. Perez, A. C. Masset, M. Hervieu, B. Raveau. A five-dimensional structural investigation of the misfit layer compound $[Bi_{0.87}SrO_2]_2[CoO_2]_{1.82}$. Acta Cryst. B 56 (2), 173–182 (2000).
7. A. Maignan, D. Pelloquin, S. Hebert, Y. Klein, M. Hervieu. Thermoelectric power in misfit cobaltites ceramics: optimization by chemical substitutions. Bol. Soc. Esp. Ceram. V. 45 (3), 122–125 (2006).
8. W. Kobayashi, S. Hebert, H. Muguerra, D. Grebille, D. Pelloquin, A. Maignan. Thermoelectric properties in the misfit-layered-cobalt oxides $[Bi_2A_2O_4]$ $[CoO_2]_{b1/b2}$ (A=Ca, Sr, Ba, b(1)/b(2)=1.65, 1.82, 1.98) single crystals. In I. Kim (Ed.), Proceedings ICT 07: Twenty-sixth international conference on thermoelectrics, Korea. 2008. pp. 117-120.
9. A. Maignan, S. Hebert, M. Hervieu, C. Michel, D. Pelloquin, D. Khomskii. Magnetoresistance and magnetothermopower properties of Bi/Ca/Co/O and Bi(Pb)/Ca/Co/O misfit layer cobaltites. J. Phys.: Condens. Matter 15 (17), 2711–2723 (2003).
10. H. Itahara, C. Xia, J. Sugiyama, T. Tani. Fabrication of textured thermoelectric layered cobaltites with various rock salt-type layers by using *b*-$Co(OH)_2$ platelets as reactive templates. J. Mater. Chem. 14 (1), 61–66 (2004).
11. A. Sotelo, G. Constantinescu, Sh. Rasekh, M. A. Torres, J. C. Diez, M. A. Madre. Improvement of thermoelectric properties of $Ca_3Co_4O_9$ using soft chemistry synthetic methods. J. Eur. Ceram. Soc. 32 (10), 2415-2422 (2012)
12. M. A. Torres, A. Sotelo, Sh. Rasekh, I. Serrano, G. Constantinescu, M. A. Madre, J. C. Diez. Improvement of thermoelectric properties of $Bi_2Sr_2Co_{1.8}O_x$ through solution synthetic methods. Bol. Soc. Esp. Ceram. V. 51 (1), 1-6 (2012)
13. A. Sotelo, Sh. Rasekh, M. A. Madre, E. Guilmeau, S. Marinel, J. C. Diez. Solution-based synthesis routes to thermoelectric $Bi_2Ca_2Co_{1.7}O_x$. J. Eur. Ceram. Soc. 31 (9), 1763-1769 (2011).
14. D. Grossin, J. G. Noudem. Synthesis of fine $La_{0.8}Sr_{0.2}MnO_3$ powder by different ways. Solid State Sci. 9 (3-4), 231-235 (2007)
15. C. S. Sanmathi, Y. Takahashi, D. Sawaki, Y. Klein, R. Retoux, I. Terasaki, J. G. Noudem. Microstructure control on thermoelectric properties of $Ca_{0.96}Sm_{0.04}MnO_3$ synthesised by co-precipitation technique. Mater. Res. Bull. 45 (5), 558-563 (2010)
16. Sh. Rasekh, M. A. Madre, A. Sotelo, E. Guilmeau, S. Marinel, J. C. Diez. Effect of synthetic methods on the thermoelectrical properties of textured $Bi_2Ca_2Co_{1.7}O_x$ ceramics. Bol. Soc. Esp. Ceram. V. 49 (1), 89-94 (2010).
17. M. A. Madre, Sh. Rasekh, J. C. Diez, A. Sotelo. New solution method to produce high performance thermoelectric ceramics: A case study of Bi-Sr-Co-O. Mater. Lett. 64 (23), 2566-2568 (2010)
18. S. Marinel, D. Bourgault, O. Belmont, A. Sotelo, G. Desgardin. Microstructure and transport properties of YBCO zone melted samples processed in a microwave cavity and infra-red furnace. Physica C 315 (3-4), 205-214 (1999).
19. W. Shin, N. Murayama. Thermoelectric properties of (Bi,Pb)-Sr-Co-O oxide. J. Mater. Res. 15 (2), 382-386 (2000).
20. J. G. Noudem, D. Kenfaui, D. Chateigner, M. Gomina. Toward the enhancement of thermoelectric properties of lamellar $Ca_3Co_4O_9$ by edge-free spark plasma texturing. Scripta Mat. 66 (5), 258-260 (2012).
21. A. Sotelo, E. Guilmeau, M. A. Madre, S. Marinel, J. C. Diez, M. Prevel. Fabrication and properties of textured Bi-based cobaltite thermoelectric rods by zone melting. J. Eur. Ceram. Soc. 27 (13-15) 3697-3700 (2007).
22. N. M. Ferreira, Sh. Rasekh, F. M. Costa, M. A. Madre, A. Sotelo, J. C. Diez, M. A. Torres. New method to improve the grain alignment and performance of thermoelectric ceramics. Mater. Lett. 83, 144-147 (2012).
23. H. Q. Liu, X. B. Zhao, T. J. Zhu, Y. Song, F. P. Wang. Thermoelectric properties of Gd, Y co-doped $Ca_3Co_4O_{9+\delta}$. Current Appl. Phys. 9 (2), 409-413 (2009).
24. A. Sotelo, Sh. Rasekh, E. Guilmeau, M. A. Madre, M. A. Torres, S. Marinel, J. C. Diez. Improved thermoelectric properties in directionally grown $Bi_2Sr_2Co_{1.8}O_y$ ceramics by Pb for Bi substitution. Mater. Res. Bull. 46 (12), 2537-2542 (2011).
25. Sh. Rasekh, M. A. Madre, J. C. Diez, E. Guilmeau, S. Marinel, A. Sotelo. Effect of Pb substitution on the thermoelectrical properties of textured $Bi_2Ca_2Co_{1.7}O_y$ ceramics prepared by a polymer solution method. Bol. Soc. Esp. Ceram. V. 49 (5), 371-376 (2010)
26. A. Sotelo, E. Guilmeau, Sh. Rasekh, M. A. Madre, S. Marinel, J. C. Diez. Enhancement of the thermoelectric properties of directionally grown Bi-Ca-Co-O through Pb for Bi substitution. J. Eur. Ceram. Soc. 30 (8), 1815-1820 (2010).
27. A. Sotelo, M. A. Torres, G. Constantinescu, Sh. Rasekh, J. C. Diez, M. A. Madre. Effect of Ag addition on the mechanical and thermoelectric performances of annealed $Bi_2Sr_2Co_{1.8}O_x$ textured ceramics. J. Eur. Ceram. Soc. 32 (14), 3745-3751 (2012)
28. A. Sotelo, M. Mora, M. A. Madre, J. C. Diez, L. A. Angurel, G. F. de la Fuente. Ag distribution in thick Bi-2212 floating zone textured rods. J. Eur. Ceram. Soc. 25 (12), 2947-2950 (2005)
29. P. Majewski, A. Sotelo, H. Szillat, S. Kaesche, F. Aldinger. Phase diagram studies in the system Ag-"$Bi_2Sr_2CaCu_2O_8$". Physica C 275 (1-2), 47-51 (1997).
30. M. A. Madre, M. A. Torres, Sh. Rasekh, J. C. Diez, A. Sotelo. Improvement of thermoelectric performances of $Bi_2Sr_2Co_{1.8}O_x$ textured materials by Pb addition using a polymer solution method. Mater. Lett. 76, 5-7 (2012)
31. A. Sotelo, Sh. Rasekh, M. A. Madre, J. C. Diez. Precursor influence on the electrical properties of textured Bi-2212 superconductors. J. Supercond. Nov. Magn. 24 (1-2), 19-25 (2011)
32. Z. Gaoke, L. Ying, Y. Xia, W. Yanping, O. Shixi, L. Hangxing. Comparison of synthesis methods, crystal structure and characterization of strontium cobaltite powders. Mater. Chem. Phys. 99 (1), 88-95 (2006).
33. M. Kato, Y. Goto, K. Umehara, K. Hirota, I. Terasaki. Synthesis and physical properties of Bi-Sr-Co-oxides with 2D-triangular Co layers intercalated by iodine. Phys. B 378-380, 1062-1063 (2006).
34. D. Mercurio, J. C. Champarnaud-Mesjard, B. Frit, P. Conflant, J. C. Boivin, T. Vogt. Thermal evolution of the crystal-structure of the rhombohedral $Bi_{0.75}Sr_{0.25}O_{1.375}$ phase - A single-crystal neutron-diffraction study. J. Solid State Chem. 112 (1), 1-8 (1994).
35. G. Becherer, R. Ifland. Über eine präzisionsbestimmung der gitterkonstanten von silber nach dem rückstrahlverfahren. Naturwissenschaft 41 (20), 471-471 (1954).
36. B. Özkurt, M. A. Madre, A. Sotelo, M. E. Yakinci, B. Özçelik. Relationship between growth speed, microstructure, mechanical and electrical properties in Bi-2212/Ag textured composites. J. Supercond. Nov. Magn. 25 (4), 799-804 (2012).
37. M. Mora, A. Sotelo, H. Amaveda, M. A. Madre, J. C. Diez, L. A. Angurel, G. F. de la Fuente. Efecto de la adición de Ag en Bi-2212 texturado mediante laser. Bol. Soc. Esp. Ceram. V. 44 (4), 199-203 (2005).
38. A. Sotelo, Sh. Rasekh, G. Constantinescu, M. A. Torres, M. A. Madre, J. C. Diez. Improvement of textured $Bi_{1.6}Pb_{0.4}Sr_2Co_{1.8}O_x$ thermoelectric performances by metallic Ag additions. Ceram. Int. 39 (2), 1597-1602 (2013)
39. T. Itoh, I. Terasaki. Thermoelectric properties of $Bi_{2.3-x}Pb_xSr_{2.6}Co_2O_y$ single crystals. Jpn. J. Appl. Phys. 39 (12A), 6658-6660 (2000).
40. W. Kobayashi, H. Muguerra, S. Hebert, D. Grebille, A. Maignan. Metallicity and positive magnetoresistance induced by Pb substitution in a misfit cobaltate crystal. J. Phys.: Condens. Matter 21, 235404 (2009).

Recibido: 10/10/2012
Aceptado: 06/03/2013